

## ANALYSIS OF THE NSLS-II MAGNET MEASUREMENT DATA\*

W. Guo<sup>†</sup>, A. Jain, S. Sharma, J. Skaritka, C. Spartaro  
BNL, Upton, NY 11973, USA

## Abstract

NSLS-II is a third generation 3-GeV light source that is scheduled to commission in the summer of 2013 at the Brookhaven National Laboratory. The 30-DBA storage ring will provide micron size beam resulting from the 1nm emittance. The magnet measurement and installation were completed in early 2013. In this paper we will introduce the main design parameters for the magnets, and present the statistical analysis of the measurement data and compare with the design tolerances.

## INTRODUCTION

NSLS-II consists of a 200 MeV linac, a 158m full energy booster, and a 792m storage ring. The storage ring has 30 double bend achromatic cells. There are 2 dipoles, 10 quadrupoles, 9 sextupoles, 6 slow correctors and 3 fast correctors in each cell. The design and specification of the magnets can be found in Ref. [1, 2, 3]. Here we present the measurement results for each type.

## DIPOLE MAGNETS

The dipoles are 2.58m long (yoke length) C-type rectangular magnets. The dipoles have a main coil, which provides 6° (104.72mr) bending, and 1% trim coil. There are two gap variants. Six dipoles have a gap size of 90mm, and the remaining fifty-four have 35mm gap. The larger gap dipoles are used to extract the infrared radiation, which are located in cell 3, 13 and 23 symmetrically. All the dipole magnets are powered in one circuit. A 100mm long removable extension piece is attached to both ends of the dipole to regulate the end fields. It was also planned to bevel the end pieces to match the edge effects; however, it was later found from measurement that the edge focusing from both types are very close to the theoretical value (i.e.,  $\theta/2\rho$ , where  $\theta=0.10472$ .) and no further machining was needed. During fabrication the difficulties were precise control of the yoke length and the vertical gap. The yoke length could vary during the stacking and curing processes, and result in variation of the integrated strength. The gap also determines the field strength. In principle the integrated strength can be controlled by the gap size, however, it becomes impractical if the magnet has to be moved back and forth between the measurement and machining setups. The gap variation along the magnet generates field fluctuation and higher-order harmonics. For example, for

the 35mm gap dipole a 35 $\mu$ m gap variation would cause  $\Delta B/B = 1 \times 10^{-3}$ . Field variation could be caused by other mechanisms, such as variation of packing density. The field variation of all the NSLS-II dipoles is <0.5mT in the specified body good field region of  $|x| < 20$ mm and  $|y| < 10$ mm at the full field of 0.4T. The dipole field is scanned by a Hall-probe arm along a pre-calculated curve. The positioning precision is  $\sim 30\mu$ m due to a feedback loop on the readout from a linear encoder attached to the track. The three vertically separated ( $\pm 10$ mm) Hall probes are calibrated against an NMR magnetic field meter. The closed orbit was found by tracking through the data using a 2nd order Runge-Kutta method. The harmonics relative to the beam orbit are then calculated at each point. Table 1 shows the statistics of the integrated field and harmonics of the fifty-four 35mm dipole magnets. The 90mm magnets have similar results. Fig. 1 is the plot of the normal quadrupole term  $b_1$  of all the 35mm dipoles. We have put these errors into simulation and found that the orbit can be corrected using the trims, and the harmonics are acceptable.

Table 1: 35mm Dipole Statistics

$\sigma_\theta/\theta$	$\langle b_1 L \rangle$	$\sigma_{b_1 L}$	$\langle b_2 L \rangle$	$\sigma_{b_2 L}$	$\langle b_3 L \rangle$	$\sigma_{b_3 L}$
	mT	mT	mT/m	mT/m	$\mu$ T/m <sup>2</sup>	$\mu$ T/m <sup>2</sup>
0.0015	24	1.9	-0.36	0.044	-0.83	2

$b_i$  is defined as  $\frac{1}{i!} \frac{\partial^i B_y}{\partial x^i}$ ,  $b_i L$  is the integration of one edge.

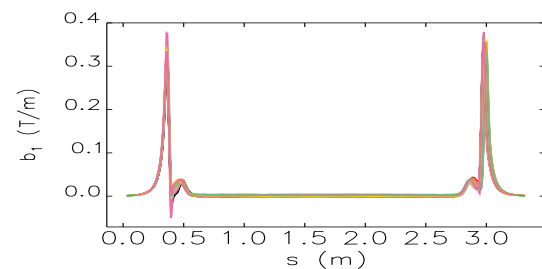


Figure 1: The quadrupole component  $b_1$  along beam orbit  $s$  of all the 35mm dipoles. The small bump is due to the extension piece.

## QUADRUPOLES AND SEXTUPOLES

There are totally 300 quadrupoles and 270 sextupoles in the storage ring, belonging to 8 and 9 families, respectively. It was pursued to reduce the number of magnet types. However, due to the lattice structure the focusing quadrupoles are stronger therefore had to be longer. Some magnets in the same family have a wider yoke to accommodate the x-ray pipes; therefore the type is doubled in such a case. There is also variation in aperture.

07 Accelerator Technology and Main Systems

T09 Room-temperature Magnets

\* This manuscript has been authored by Brookhaven Science Associates, LLC under Contract No. DE-AC02-98CH1-886 with the U.S. Department of Energy.

<sup>†</sup> wguo@bnl.gov

The larger aperture magnets are designed to provide a larger good field region for places where dispersion reaches the peak value. The magnet family, aperture, length and maximum strength are listed in Table 2.

Table 2: NSLS-II Multipole Main Parameters

Magnet families	D (mm)	$L_M$ (mm)	$n!b_nL$
QH1/3, QL1/3	66	270	5.5 T
QH2, QL2	66	440	8.8 T
QM1	66	247	2.75 T
QM2	90	277	3.79 T
SH1-4, SL1-3, SM1	68	200	80 T/m
SM2	76	248	100 T/m

Quadrupoles start with Q, and sextupoles start with S. D is the bore diameter,  $L_M$  is the magnetic length and  $n!b_nL$  is the maximum integrated strength.

The quality issues for the multipole manufacturing is mostly on the harmonics. NSLS-II magnets are required by contract to meet the specifications. A well-designed profile can minimize the symmetry-allowed harmonics; however, assembly error and structural asymmetry will produce low order harmonics, such as octupole and decapole terms. These terms differ from magnet to magnet and must be compensated individually. Iron shims several tens of microns thick are put between the mating surfaces to restore the symmetry and compensate for these low order harmonics. Some other approaches, such as pole chamfering, are also effective in reducing these harmonic terms.

There were two concerns about the transfer function. At NSLS-II one fifth of the sextupoles in one family are powered by one power supply; therefore the strength uniformity was a concern. To make it even worse the wide (9802) and the normal (9801) sextupoles built by different manufacturers are configured in one family. Simulation shows a 0.5% (rms) variation is tolerable. Figure 2 shows the integrated strength at a fixed current for the two types of sextupoles. Even though there is an apparent difference among the two types, the majority of the magnets still meet the  $\pm 0.5\%$  requirement. The magnets with large deviations were set apart as spares.

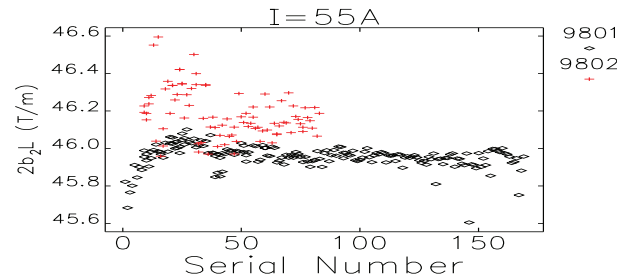


Figure 2: The integrated strength ( $2b_2L$ ) at  $I=55A$  for 9801 and 9802 sextupoles.

All quadrupoles are powered independently; hence transfer function uniformity is not a concern. However, we are still concerned about the linearity of the magnets. Shown in Fig.3 is the ratio of the integrated strength to current. It is a constant if the magnet was perfectly linear.

In practice the ratio is nonlinear at low current end due to residual field, and also at high current due to iron saturation. By comparing Fig. 3 and the upper plot in Fig. 4 we observe the correlation between magnet saturation and field deterioration. QDP-9804 are the focusing magnets therefore the gradient is large. The ratio change is less than 5%, which is not a problem because we found the field quality is still acceptable. The change is smaller for the defocusing magnets due to smaller field gradient.

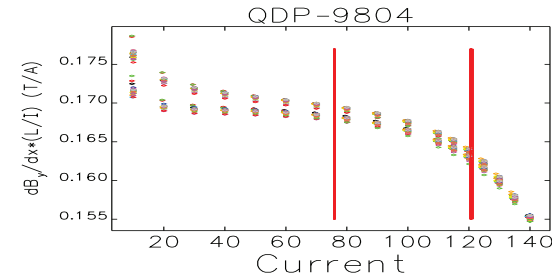


Figure 3: Integrated strength normalized by current for quadrupole 9804. The red lines indicate the tuning range.

The results of the harmonics are shown in the following figures. Fig. 4 is a comparison of the typical behavior of low order and high order harmonics. It can be seen that the low order harmonics vary with current, and fluctuate among magnets; however the high order harmonics are usually small and current-independent. The harmonics are defined as  $B_m = r_0^m b_m / (r_0^n b_n)$ , where  $b_m = \frac{1}{m!} \frac{\partial^m B_y}{\partial x^m}$ ,  $b_n$  is the main field. Both  $b_m$  and  $b_n$  are evaluated at the reference radius  $r_0 = 25mm$ . In the figures 4 to 6 all the harmonics are in units of  $10^{-4}$ .

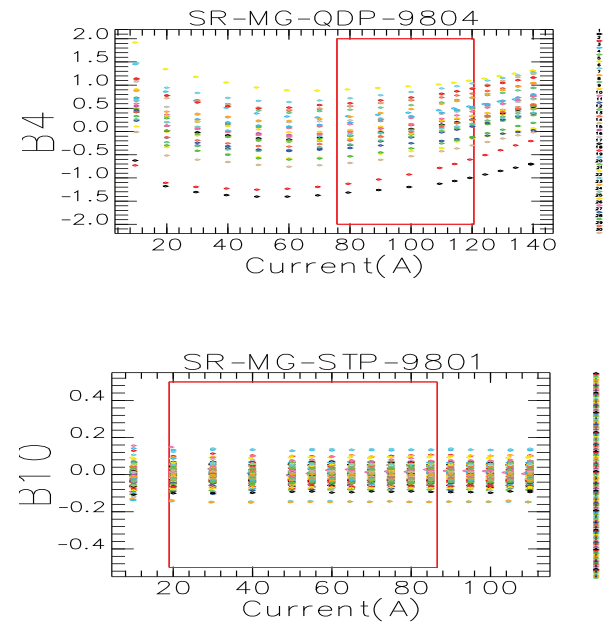


Figure 4: A typical low (upper) and high (lower) order harmonics. The red rectangle indicates tuning range and specification. The colors correspond to different magnets.

Figure 5 shows the specification, the average value and the standard deviation ( $2\sigma$ ) of the measured harmonics of

all the 66mm quadrupoles. Figure 6 shows the same results for the sextupoles. Most of the harmonics stay in spec, except for a few low order and symmetry-allowed terms. The effects of harmonics on the beam dynamics can be found in [3]. The actual harmonics will be put into the lattice model; however, we expect the impact on the accelerator performance is acceptable.

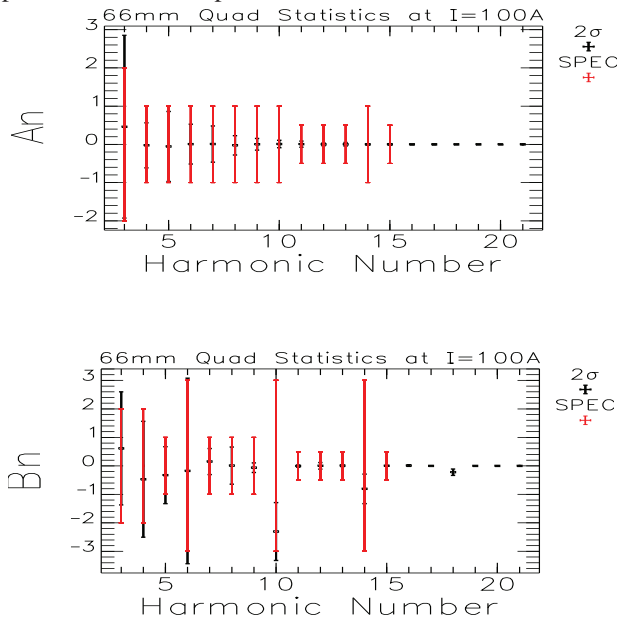


Figure 5: Statistics of skew (upper) and normal (lower) harmonics of 66mm quadrupole at I=100A.

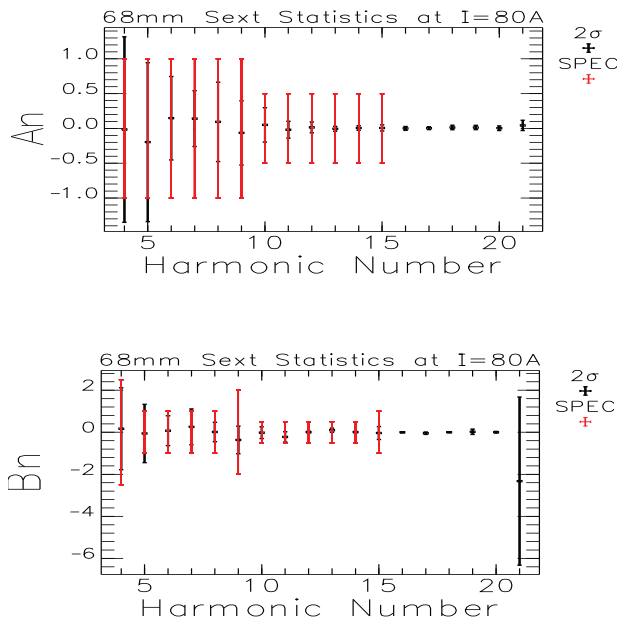


Figure 6: Statistics of skew (upper) and normal (lower) harmonics of 68mm sextupole at I=80A.

### CORRECTOR MAGNETS

There are three types of slow correctors, owing to different apertures and functions. The type A corrector will

be placed over the bellows therefore the aperture is larger (156mm). The 100mm type C corrector will be installed on the multipole aluminum vacuum chambers, and the type D corrector has the same structure as type C, except that a pair of race-track coils for skew quadrupole are affixed to the upper and lower poles. The good field region of the correctors are specified as  $|x| < 15\text{mm}$ , and  $|y| < 10\text{mm}$ . In the good field region the field variation is designed to be less than 1%. The key parameters are shown in Table 3. The typical result of measured harmonics are shown in Table 4. Due to the six pole design [4] the odd order harmonics are large for the horizontal field mode. Even though the harmonics have large relative values, the actual effects are small due to limited strength of the correctors.

Table 3: NSLS-II Corrector Main Parameters

Type	Aper.(mm)	$L_M$ (mm)	BL
A (H/V)	156	300	0.0088 Tm
C (H/V)	100	200	0.008 Tm
D (H/V)	65	200	0.008 Tm
D (Skew Quad)	65	n/a	0.0072 T

Table 4: Large Harmonics of Corrector #6 of Type C

$B_x$	$a_1$	$a_3$	$a_4$	$a_5$	$a_7$	$b_1$	$b_3$	$b_5$
	10000	-204	16	-179	19	-65	4	5
$B_y$	$b_1$	$b_2$	$b_3$	$b_4$	$b_5$	$b_7$	$a_1$	$a_3$
	-10000	32	50	3	-28	4	-56	1

The air-cooled fast correctors will be installed over inconel vacuums chambers. The chamber dimension is 25x75mm and the coil separation is 27x78mm. The good field region is defined as  $|x| < 4\text{mm}$  and  $|y| < 2\text{mm}$ , with a specified  $< 1\%$  strength variation. The maximum strength is  $15 \mu\text{r}$  at 0.1Hz. The phase shift is  $5^\circ$  up to 1kHz with the vacuum chamber, however the strength will be slightly lower at higher frequencies due to inductance and eddy currents.

### SUMMARY

We have presented the designed and the measured main parameters of the NSLS-II magnets. Particularly we showed the strength variation and field quality of the dipole, quadrupole and sextupole magnets. The designed strength and the measured harmonics are also shown for the correctors. All the accepted magnets meet the NSLS-II requirements and specifications.

### REFERENCES

- [1] Skaritka et al, "The Design and Construction of the NSLS-II Magnets," Proceedings of PAC'09, p145.
- [2] W.Guo et al, "Physics Considerations and Specifications for the NSLS-II Magnets," Proceedings of IPAC'10, p2666.
- [3] W.Guo et al, "Re-examination of the NSLS-II Magnet Multipole Specification," Proceedings of PAC'11, p1531.
- [4] G.Danby et al, Proc. PAC'09, p148-150.